Title

Paleointensity determination from São Miguel (Azores Archipelago) over the last 3ka

Journal

Physics of the Earth and Planetary Interiors, 234

ISSN

0031-9201

Authors

Di Chiara, A
Tauxe, L
Speranza, F

Publication Date

2014

DOI

10.1016/j.pepi.2014.06.008

Peer reviewed

Physics of the Earth and Planetary Interiors 234 (2014) 1–13

Contents lists available at ScienceDirect

Physics of the Earth and Planetary Interiors

journal homepage: www.elsevier.com/locate/pepi

Paleointensity determination from São Miguel (Azores Archipelago) over the last 3 ka

Anita Di Chiara [a,b,c,*], Lisa Tauxe [d], Fabio Speranza [a]

[a] Istituto Nazionale di Geofisica e Vulcanologia, via di Vigna Murata 605, Roma, Italy
[b] University of Bologna, Bologna, Italy
[c] Universidade de São Paulo, IAG, Rua do Matão 1226, SP, Brazil
[d] Geosciences Research Division, Scripps Institution of Oceanography, La Jolla, CA, 92093-0220, United States

ARTICLE INFO

Article history:
Received 11 February 2014
Received in revised form 23 May 2014
Accepted 3 June 2014
Available online 16 June 2014

Keywords:
Paleomagnetism
Paleointensity
Azores
Atlantic Ocean
Geomagnetic field intensity spike

ABSTRACT

Paleointensity data from the Atlantic Ocean are rare. We present new paleointensity data from São Miguel (Azores Islands, Portugal) based on 20 paleomagnetic sites from 13 lava flows emplaced over the last 3000 years. Ten lava flows are radiocarbon dated, whereas three flows were paleomagnetically dated and one site was dated using stratigraphic relations. All the samples, previously investigated to recover paleodirections, were subjected to IZZI experiments. Importantly, the new data are internally consistent, agree with Moroccan and European datasets, and offer new constraints for global geomagnetic field models. Some of the ages of the paleomagnetically dated lava flows have been revised based on the intensity data presented here. The inferred Virtual Axial Dipole Moments (VADMs) range from 68.2 to 163.5 ZAm^2. A peak in field strength with an estimated age of around 600 BC is well supported by two sites from the same flow (Furna), and is comparable to the high intensity values found in Portugal for the same age and the earlier field peak at about 1000 BC in the Levant. A gradient in VADM values with latitude from northwestern Africa and across Europe between 100 and 1000 AD is confirmed as well as its absence from between 0 to 100 AD.

1. Introduction

The modern geomagnetic field is dominated by a geocentric axial dipole but there are significant departures from the simple bar magnet model. These manifest themselves in part, as large patches of anomalous behavior, known as "flux patches". There are currently two of these positive anomalies in the northern hemisphere, one over Eurasia and one over North America (lower inset to Fig. 1).

Direct measurement of intensities began in 1840 AD (when C. F. Gauss devised the first method to measure it), whereas measurement of directions (declination and/or inclination) are available since before 1600 AD. Jackson et al. (2000) combined the global model directions with a linear extrapolation of paleomagnetic intensity measurements to estimate the strength of the magnetic field over the period since 1600 AD, and produced a time dependent spherical harmonic field model for that time period (GUFM). To understand the longer term behavior of the geomagnetic field, we rely on paleo- and archeomagnetic studies.

The GEOMAGIA database was created by Donadini et al. (2006), then expanded (Donadini et al., 2009) and is updated periodically; it contains archeointensity, and paleointensity data from volcanics, as well as directions. The temporal and geographical distribution of data is uneven. For the last 10 kyr, a large amount of data has been published from continents with the majority coming from Europe. While there have been several recent studies as far west as Portugal (Nachasova and Burakov, 2009; Hartmann et al., 2009), and Morocco (Kovacheva, 1984; Gómez-Paccard et al., 2012), the central-northern Atlantic Ocean is, apart from historical (Michalk et al., 2008) and post-glacial lavas from Iceland (Schweitzer and Soffel, 1980; Stanton et al., 2011; Tanaka et al., 2012), essentially devoid of data. Consequently, global models (e.g., CALSxk.x family, ARCH3k and SHA.DIF.xk) have very few constraints from the central northern Atlantic (Korte et al., 2009; Donadini et al., 2009; Korte and Constable, 2011; Genevey et al., 2008; Pavón-Carrasco et al., 2014).

In contrast to the central northern Atlantic data sets, there is a robust and rapidly growing one for Europe. Particular features in the secular variation models, likely representing the growth and

* Corresponding author at: Universidade de São Paulo, IAG, Rua do Matão 1226, SP, Brazil. Tel.: +55 11950594087.
E-mail addresses: dichiaraanita@gmail.com (A. Di Chiara), ltauxe@ucsd.edu (L. Tauxe), fabio.speranza@ingv.it (F. Speranza).

http://dx.doi.org/10.1016/j.pepi.2014.06.008
0031-9201/

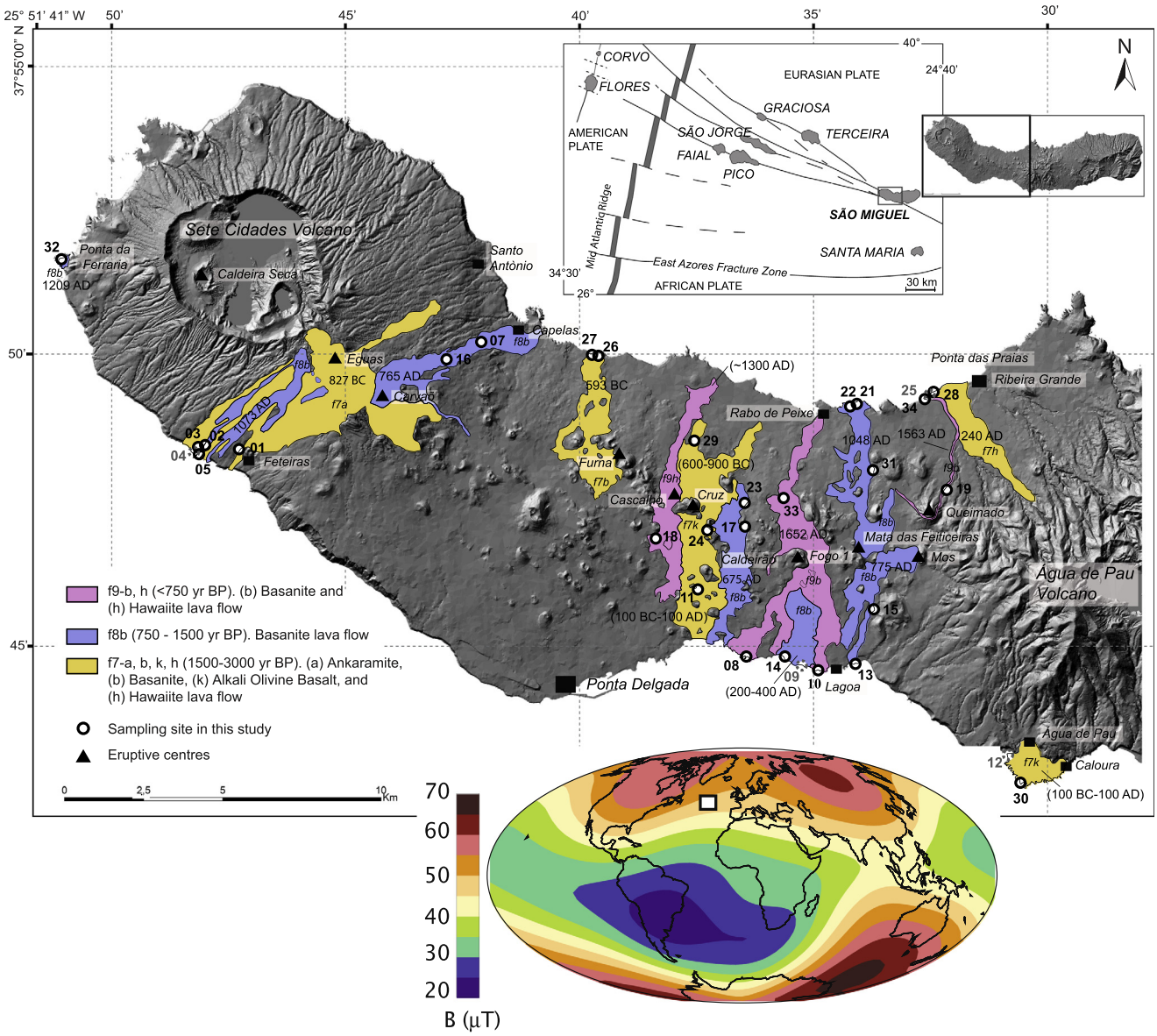

Fig. 1. Location of sampling sites of studied flows in São Miguel (Azores Archipelago, Portugal) showed in the Digital Elevation Model. The "Sml" prefix of each site is omitted. Flow geometry, characteristics, and ages are after Moore (1990, 1991). The 1563 and 1652 AD flows are historic. Calendar ages of the other lava flows were calibrated by us using CALIB6.0 (http://calib.qub.ac.uk/calib/calib.html) from original ^{14}C ages reported by Moore and Rubin (1991). Flow ages indicated with parentheses were paleomagnetically inferred (Di Chiara et al., 2012). Grey symbols of paleomagnetic sites indicate that all the samples from that site were rejected from paleointensity analyses. The inset represents the present day geomagnetic field "flux patches", arising from the non-axial dipole component. There are two of these positive anomalies in the northern hemisphere, one over Eurasia and one over North America.

decay of flux patches are well constrained and reproduced by several different studies from different regions. Between 2500 and 3000 years ago, a rapid change in intensity was recorded in Europe (Gallet and Le Goff, 2006; Ben-Yosef et al., 2008; Genevey et al., 2009), reaching the highest values in the Southern Levant area (Ben-Yosef et al., 2009) of up to 213.1 ZAm^2 between 816 ± 17 BC and 983 ± 25 BC. Recently, data from the Balkan area (80 μT, or 173.3 ZAm^2 dated at around 500 BC; Tema and Kondopoulou, 2011) confirm the high value, whereas data from Italy (Tema et al., 2013) are too scattered to confirm the possible spike. High field values for the same period were obtained from the Western US (Champion, 1980; Hagstrum and Champion, 1994) (values up to 140 ZAm^2), and even higher values of up to 200 ZAm^2 from Hawaii (Pressling et al., 2006) (although these were not reproduced in the later studies of Pressling et al., 2009). And recently, values of around 130 ZAm^2 were observed at about 1320–1380 BC in Korea by Hong et al. (2013). These data suggest the possibility of a high dipolar field at that time, and encourage further investigations of the regional extent of this feature (or these features). Another short period of high intensity occurring 1000 years ago was observed in the central Pacific, Hawaii (DeGroot et al., 2013), which is qualitatively similar to behavior observed 200 years earlier in Europe and 500 years later in Mesoamerica. Our data serve to place these discoveries in a larger context.

The Azores Archipelago is an ideal location for gathering new paleointensity data, as historical and pre-historical lava flows are well exposed and geochronologically dated (e.g., Feraud et al., 1980; Moore, 1990, 1991; Moore and Rubin, 1991). A paleosecular variation curve (PSV) was obtained based on 16 lava flows emplaced over the last 3 kyr on São Miguel (Di Chiara et al., 2012). The PSV curve was reconstructed using 27 radiocarbon dated sites from 16 lava flows, together with 6 directions gathered

by Johnson et al. (1998). Sister specimens from the same samples from sites investigated by Di Chiara et al. (2012) were analyzed in this study, in order to obtain new paleointensity data.

2. Geological setting and studied lava flows

São Miguel is the largest (760 km^2) of the nine volcanic islands of the Azores Archipelago, straddling the Mid Atlantic Ridge at the triple junction of the North American, Eurasian and African plates (Fig. 1). Four large trachytic stratovolcanoes developed from 8.1 Ma (Abdel-Monem et al., 1975; Feraud et al., 1980) to historical times. From east to west, six volcano-stratigraphic units had been recognized: Nordeste, Furna, the plateau do Congro, Agua de Pau, Região dos Picos, and Sete Cidades Volcano. The "Região dos Picos" (Moore, 1990, 1991) is a flat area of basaltic lava flows speckled with volcanic cones and is the most populated. Two historical eruptions occurred on the island, both located in the central part and the eastern part of the Região dos Picos. The Fogo eruption in 1563 AD was the most recent high explosive (subplinian) eruption at Fogo inland and at Fogo caldera. It also produced two thin lava flows originating from the monogenetic Queimado cone, nearby to the Ponta das Praias locality (f5b in Fig.1). The other historical eruptive event was the most recent inland effusive eruption, which was emplaced from the Fogo 1 cone in 1652 AD (unit f9b on Fig. 1). This flow reached both the northern coast (at Rabo de Peixe town) and the southern coast near the town of Lagoa. The two historical flows are described in chronicles by Mitchell-Thomè (1981) and Booth et al. (1978). For older flows, boundaries were delimited on the geological map of Moore (1990) based on field evidences. Satellite images were of little use as only small scoria cones dotting the area are evident and the lava flow limits are covered by vegetation and by human colonization.

We sampled the two historical lava flows in July 2010, as well as an additional 32 paleomagnetic sites, with at least 15 well-spaced cores at each site. Cores were oriented both by solar and magnetic compass. In all, we sampled 16 flows at 35 sites as described in Di Chiara et al. (2012; Fig. 1 and Table 1 in Di Chiara et al., 2012). These span an age range between 3 ka and 1652 AD. Seven sites from some of the same flows were also investigated paleomagnetically by Johnson et al. (1998). Combining the two studies, 31 sites yielded reliable paleomagnetic results. All the pre-historical radiocarbon ages reported by Moore (1990, 1991) and Moore and Rubin (1991) were recalibrated by us with the Stuiver's Online program Calib6.0 (Stuiver et al., 2009). An additional four of the 16 sampled flows were dated using the comparison of the paleomagnetic directions (see Table 2 in Di Chiara et al., 2012): Cruz N and S, Lagoa, and Caloura flows (marked in Table 1) with recalculated reference curves. Recently, it was suggested that paleointensity estimates could be used in conjunction with geomagnetic global field models (e.g., Jackson et al., 2000; Korte and Constable, 2011) to help constrain eruptive ages for young lavas (Carlut and Kent, 2000; Gee et al., 2000; Carlut et al., 2004; Bowles et al., 2005). We explore the latter in Section 4.2.

3. Methods

To achieve our purpose, we first tackled the methodological issue of what is the optimal method by which to recover the paleointensity of the Earth's magnetic field. Indeed, over the past forty years a large number of techniques have been proposed to improve the quality and reduce the time of experiments for absolute paleointensity (e.g., Coe et al., 1978; Shaw, 1974; Hoffman et al., 1989; Tauxe and Staudigel, 2004; Dekkers and Böhnel, 2006; see review by Tauxe and Yamazaki, 2007). Despite (or because) of these efforts, there remains no consensus on the best method. Therefore, some procedures remain controversial and poorly tested.

The Thellier family of experiments (e.g., Thellier and Thellier, 1959) is by far the most accepted and widely used method to recover paleointensities. It is based on three main assumptions: (1) a linear relationship exists between the geomagnetic field and the thermal remanent magnetization (TRM); (2) during the experiments no alteration of the ability to acquire thermal remanence occurs and normalization of the natural remanent magnetization (NRM) with a laboratory TRM yields an accurate estimate for ancient field strength; (3) the temperature at which a partial thermal remanence is blocked is the same as that which it is unblocked. The third assumption has been verified for single domain materials, but frequently fails for multi-domain remanences. Given these constraints, suitable materials are rare: we require an original component of NRM, carried by single domain ferromagnetic minerals, with no evidence of alteration during laboratory analysis. Therefore, one of the best approaches for testing the validity of the absolute paleointensity determination is to deal with quickly cooled lava flow deposits (e.g. Pan et al., 2002) and basaltic glasses (Pick and Tauxe, 1993; Ferk et al., 2008; Cromwell et al., 2011). Many cross-tests of the different techniques on historical flows of measured intensity have been carried out in order to assess various techniques and to identify the best method. For instance, at least nine studies have focused on the 1960 lava flow from the Big Island of Hawaii (Abokodair, 1977; Tanaka and Kono, 1991; Tsunakawa and Shaw, 1994; Tanaka et al., 1995; McCLelland and Briden, 1996; Valet and Herrero-Barvera, 2000; Hill and Shaw, 2000; Yamamoto et al., 2003; Herrero-Bervera and Valet, 2009); these studies are marked by their inability to recover the ancient magnetic field accurately. More recently however, Cromwell et al. (2012) have achieved an unprecedented accuracy in recovering the historical field from the 1960 and other historical lava flows by sampling the finest grained (glassy) portions of the flow and using the IZZI method of Tauxe and Staudigel (2004). We therefore use the IZZI protocol in this study.

The IZZI protocol is a combination of two versions of the original method, one proposed by Aitken (1988; in-field, zero-field; IZ) and one by Coe (1967; zero-field, in-field; ZI), thus it alternates the IZ and ZI steps, and adds a pTRM check step after every ZI step. The advantages of this technique are triple: (1) the angular dependence between the Natural Remanent Magnetization (NRM) and the TRM acquired during experiments under a known laboratory field (TRM_{lab}) can be easily detected, indicated as an angle θ; (2) it provides a quantitative estimate for the consistency of the outcome between IZ and ZI steps thereby allowing detection of so-called pTRM tails that bias paleointensity results; (3) it is quicker and requires fewer laboratory heatings because the "pTRM tail check" of Riisager and Riisager (2001) is unnecessary.

Results are classically displayed and analyzed through the Arai plot (Nagata et al., 1963), a scatter plot displaying residual NRMs ('NRM remaining') versus cumulative pTRMs. If the material fulfills the assumptions underlying the Thellier method (i.e. the NRM is a pure TRM carried exclusively by stable SD), then the Arai plot is a straight line, connecting the two (x, y) endpoints: (0, NRM), and (TRM, 0). The most common approach for calculating the true intensity of the paleomagnetic field is the best-fit line. Some authors tend to use only the low-temperature slope while others argue that the low-temperature slope can significantly overestimate the true field (e.g. Biggin and Thomas, 2003; Calvo et al., 2002; Chauvin et al., 2005). Some authors suggest averaging the slope of the two segments (e.g. Hill and Shaw, 2000), and others recommend using as large a segment as possible even if it is curved (e.g. Levi, 1977; Biggin and Thomas, 2003; Chauvin et al., 2005). An alternative option is using only the two end-points of the Arai plots when specimens show little signs of alteration (e.g. Coe et al., 2004; Garcia et al., 2006).

Table 1
Location of sampling sites at São Miguel.

Flow name	Site	Lat. (N)	Lon. (W)	Age Uncalibrated (years BP)	Age (years ± AD)
Furna	Sml26	37.832	25.661	2460 ± 220	593 ± 236 BC
	Sml27	37.832	25.659		
Cruz N	Sml29	37.807	25.626	1500–3000	400–700 BC*
Caloura	Sml30	37.708	25.511	1500–3000	0–200 AD*
Cruz S	Sml11	37.764	25.620		0–200 AD*
Lagoa	Sml14	37.744	25.594	750–1500	100–400 AD*
Ponta das Praias	Sml28	37.819	25.540	1790 ± 150 AD	240 ± 168 AD
	Sml25	37.819	25.540		
Caldeirão	Sml17	37.782	25.608	1350 ± 120 AD	675 ± 107 AD
Caldeirão E	Sml23	37.789	25.609		
Caldeirão W	Sml24	37.780	25.621		
Carvão	Sml07	37.835	25.702	1280 ± 150 AD	765 ± 132 AD
	Sml16	37.829	25.714		
Mos	Sml13	37.742	25.569	1250 ± 150 AD	775 ± 124 AD
	Sml15	37.758	25.561		
Mata das Feiticeiras	Sml21	37.817	25.567	1010 ± 120 AD	1048 ± 113 AD
	Sml22	37.816	25.569		
Feteiras	Sml01	37.801	25.801		1073 ± 90 AD
	Sml02	37.801	25.801		
	Sml03	37.804	25.804		
	Sml05	37.803	25.803		
Cascalho	Sml18	37.779	25.643	Less than 500 ± 100 and 663 ± 105 AD	1300–1500 AD**
Ponta da Ferraria	Sml32	37.861	25.854	840 ± 60 AD	1209 ± 53 AD
Queimado	Sml19	37.792	25.535		1563 AD
	Sml31	37.798	25.562		
	Sml34	37.818	25.542		
Fogo 1	Sml10	37.740	25.582		1652 AD
	Sml33	37.790	25.594		
Fogo 1X	Sml08	37.740	25.608		

Site coordinated were gathered by a Garmin GPS using WGS84 datum. Units and uncalibrated ^{14}C ages with an error of 1s are from Moore (1990, 1991) and Moore and Rubin (1991).
* Flows whose age is defined by an age interval.
** Flose whose age was paleomagnetic dated by Di Chiara et al. (2012). Calendar ages were calibrated using the Stuiver's program CALIB6.0 Online [http://calib.qub.ac.uk].

Table 2
Threshold values of quality criteria.

Sample criteria			Specimen criteria						
N	σ (%)	σ (μT)	N	β	DANG	SCAT	FRAC	int_{mad}	N_{ptrm}
3	15	5	3	0.1	10	True	0.85	10	2

Quality parameters: n is the minimum number of samples or specimen, β is a scatter parameter, DRATS is the Difference of the RATio Sum (Tauxe and Staudigel, 2004).

The difficulty of interpretation arises from the multiple causes of failure that can affect results, causing a shift from an ideal straight line: (i) multi-domain (MD) grains can cause concave, or convex, or 'S-shaped' curves (see Levi, 1977; Xu and Dunlop, 1995, 2004; Biggin and Thomas, 2003; Coe et al., 2004; Fabian, 2001; Leonhardt et al., 2004) in the Arai Plot; and (ii) the difference of direction between the NRM with respect to the laboratory field applied during Thellier experiments (Xu and Dunlop, 2004; Fabian, 2001; Leonhardt et al., 2004; Biggin, 2006, 2010; Biggin and Poidras, 2006; Shaar et al., 2011), expressed as an angle θ, which likely is responsible for the zig-zagged behavior (when the NRM is perpendicular to the laboratory field the deviation is high).

Zigzags are unique features of the IZZI protocol (Tauxe and Staudigel, 2004; Yu et al., 2004; Yu and Tauxe, 2005; Shaar et al., 2011), and they occur when the IZ and the ZI data points create two distinct curves. Several attempts to quantify the zigzagging have been proposed (e.g. Granot et al., 2006; Tauxe, 2009). Following these findings, Shaar et al., 2011 performed experiments to demonstrate that experimental conditions can influence paleointensity experiments. In particular, factors that play an important role are the difference of the intensity of the field laboratory (B_{TRM}), and the original NRM of the sample (B_{NRM}), and the angle between B_{TRM} and B_{NRM} (θ). Linear curves can occur when $\theta = 0°$ and $B_{TRM}/B_{NRM} = 1$, while semi-linear curves with a weak zigzag occur when $\theta = 0°$ and $B_{TRM}/B_{NRM} \leqslant 2$. Concave curves occur when $\theta = 180°$, regardless the ratio B_{TRM}/B_{NRM}. Convex curves occur when $\theta = 0°$ and $B_{TRM}/B_{NRM} = 4$. The two endpoints of a non-linear plot (concave or convex) connected together yield the ideal SD line. For the same B_{TRM}/B_{NRM} the zigzag is weak for $\theta = 0°$ and strong for $\theta = 180°$. Convex curves in the Arai plots result when the field in the paleointensity oven is stronger than the ancient field. These effects are thought to be responsible for an underestimation or overestimation of the paleointensity.

As a result of experimental complications, a key problem is to adequately choose the criteria by which individual results are selected or rejected. Again there is little consensus (e.g. Biggin and Thomas, 2003; Kissel and Laj, 2004; Selkin and Tauxe, 2000; Tauxe, 2009; Shaar and Tauxe, 2013) and cut-off values of the selection statistics vary greatly among various studies.

Here, we test various suggestions for enhancing the IZZI method (by Tauxe and Staudigel, 2004; Valet et al., 2010; Shaar et al., 2011; Tanaka et al., 2012). We hoped to carefully screen all the samples in a preliminary step and reject all that do not fulfill the assumptions underlying the technique (a single-component TRM carried by SD magnetic particles that do not alter during experiments). Thus, all the samples that do not fulfill the assumptions underlying the technique and diverge from an ideal behavior of a single-component of TRM, carried by SD magnetic particles that do not alter during experiments, were excluded from paleointensity experiments (as suggested by Valet et al., 2010). The aim is to minimize the source of bias affecting the success of paleointensity results, for example samples that displayed evidence of multi-component NRM. Hence, we selected those samples (1) with no evidence of secondary remagnetizations, (i.e., those with a Zijderveld diagram trending straight

to the origin), (2) displaying "square-shouldered" blocking temperature spectra (thought to minimize the presence of MD grains), and (3) displaying reversible features on the susceptibility-temperature curves (previously obtained from all the samples), as well as those revealing a single Curie Temperature. Indeed, as particle size increases (Carlut and Kent, 2000) and MD grains are a predominant carrier of the remanent magnetization (Levi, 1977; Fabian, 2001; Riisager and Riisager, 2001; Leonhardt et al., 2004), the Arai plots tend to have a non-linear behavior and cause the failure of the experiments. Using these guidelines, all the samples previously thermally-treated to recover paleomagnetic directions (Di Chiara et al., 2012) were screened and samples displaying non-ideal behavior were rejected from any further analysis.

From the 390 samples from 33 sites that yielded reliable paleodirections after the thermal demagnetization cleaning analyses (Di Chiara et al., 2012), only 64 samples from 28 sites passed the first rigorous pre-selection step, and were subjected to paleointensity experiments. From each sample, 2 to 6 fresh sister specimens were chosen and a total of 180 specimens were prepared for the paleointensity experiments. Individual chips were placed in clean glass vials and fixed into position with microfiber glass filters and Kasil "glue". The paleointensity experiments were carried out using the in-field, zero-field, zero-field, in-field (IZZI) protocol (Tauxe and Staudigel, 2004). The protocol was carried out as follows: specimens placed in the glass vials were heated to 100 °C and cooled in zero field (Zero-field step); after measuring the remaining NRM, specimens were reheated to 100 °C and cooled in laboratory field, directed along the Z axis and re-measured (In-field step). The difference between the first NRM and the second step is the partial TRM (pTRM) gained by cooling from 100 °C to room temperature. At each subsequent temperature step, the order of the double heating procedure was reversed such that specimens were cooled in-field (I) first, then in zero-field (Z) (Zero-field/In-field, ZI, and In-field/Zero-field, IZ). The so-called pTRM check step consists of going back to the previous heating step and repeating the in-field heating in order to check if the ability of the specimen to acquire pTRM changed during the intervening heating steps. The procedure consists of a total of 43 heating steps alternating IZ and ZI and the pTRM checks, in 100 °C intervals up to 300 °C, 50 °C intervals up to 500 °C and 10 °C intervals up to 600 °C. All the experiments were performed in the shielded room of the paleomagnetic laboratory of The Scripps Institution of Oceanography (La Jolla, California, US) using double shielded water-cooled ovens for paleointensities and the 2G cryogenic magnetometer.

In order to test whether the orientation of the NRM parallel to the laboratory field affects the robustness of the results (as suggested by Fabian, 2001; Leonhardt et al., 2004; Xu and Dunlop, 2004; Yu et al., 2004; Biggin, 2006, 2010; Biggin and Poidras, 2006; Shaar et al., 2011) two separate types of experiments were performed. In one type, a total of 90 sister specimens were oriented by placing them in vials, with their NRM directions quasi parallel to the applied field direction, thus with a specimen remanent inclinations between −70° and −89° (that is parallel to *z*-axis of the 2G cryogenic Magnetometer). The remaining 90 specimens were randomly oriented with respect to the laboratory field.

Many authors stressed the importance of choosing a laboratory field equal to or slightly lower than the expected paleofield (e.g., Shaar et al., 2011; Paterson et al., 2012). The expected value of the field (Korte et al., 2011) averaged for the different ages of our samples is about 40 μT, so we chose 40 μT as the laboratory field.

In addition to the paleointensity experiments, we also carried out routine magnetic analyses on 30 specimens (about one per site) to characterize the magnetic mineralogy. Hysteresis properties were measured using a Princeton Measurement Corporation MicroMag alternating gradient magnetometer (AGM, model 2900) with a maximum applied field of 1 T. The measured hysteresis parameters include saturation magnetization (Ms), saturation remanent magnetization (Mrs), coercivity (Bc) and the coercivity of remanence (Bcr). The ratios between Mr/Ms and Bcr/Bc were plotted in a Day diagram (Day et al., 1977) in Fig. 2; representative hysteresis loops are shown in Fig. 3.

4. Results

4.1. Magnetic mineralogy

In Fig. 2 we plot hysteresis ratios of saturation remanence to saturation magnetization (Mr/Ms) and coercivity of remanence to coercivity (Bcr/Bc) for the Azores sample collection as blue squares. The Mr/Ms versus Bcr/Bc data plot in a swath well displaced from the linear SD–MD mixing curve (e.g., Dunlop, 2002; Dunlop and Carter-Stiglitz, 2006) shown as the solid red line. The theoretical curve is calculated using the SD and MD end-members from CS912 and 041183 in Dunlop and Carter-Stiglitz (2006) respectively in the equations suggested by Dunlop (2002). Our data do not follow the theoretical curve for SD–MD mixing; instead, the data are quite similar to those measured on submarine basaltic glasses by Tauxe et al. (1996), modeled as mixtures of multi-axial SD and superparamagnetic (SP) particles (Tauxe et al., 2002).

We show hysteresis loops for three representative flows (Mos: Sml1507b, Furna: Sml2614a and Feteiras: Sml0511b) in Figs. 3a–c. Fig. 3a is characteristic of single domain (SD) magnetic assemblages (or nearly so), with a Mr/Ms ratio of 0.47. The behavior shown in Fig. 3b is not pure SD but appears to be slightly 'wasp-waisted', indicating a mixture of SD and SP (Pick and Tauxe, 1993). Fig. 3c is ambiguous, and could be an assemblage of so-called 'pseudo-single domain' (PSD) grain sizes with vortex structures in their remanent state, or nearly multidomain (MD) assemblages. Fig. 3d–f show representative stepwise thermal demagnetization curves for sister specimens from the same flows as those shown in Fig. 3a–c. In the first two demagnetization curves (Fig. 3d and e), the fractional magnetization drops over a narrow range of temperatures, close to the Curie point, displaying a coherent trend among all specimens from the same flow. Thus between 60% and 80% of the remanence unblocks above temperatures of 400–500 °C, consistent with the suggestion of dominantly single domain behavior from the hysteresis loop shown in Fig. 3a. Fig. 3e drops in a slightly more gradual fashion than Fig. 3d. Fig. 3f shows at least one specimen that demagnetizes over a more distributed range of blocking temperatures. Lower blocking temperatures can be the result of grains near the SP/SD threshold size, or could result from PSD grains. Based on the behavior during the paleointensity experiments discussed in the following, we suggest that the slightly wasp-waisted loop, coupled with slightly lower blocking temperatures shown in Fig. 3b and h reflect a grain size distribution that spans the SP/SD range, and the behavior shown in Fig. 3c and f results from a distribution including larger PSD grains.

The behavior of specimens during the paleointensity experiment associated with the three styles of hysteresis loops is illustrated in the bottom panel of (Fig. 3g, h, i). In the case in which the hysteresis behavior is close to an ideal SD assemblage, and the blocking temperature spectra drops near the Curie point of magnetite (Fig. 3a and d) the specimens behave very well during the paleointensity experiment (Fig. 3g). On the contrary, the hysteresis behavior shown in Fig. 3c, which may reflect coarser grain sizes is associated with less than ideal behavior during the paleointensity experiment (Fig. 3f and i).

We find that when magnetic mineralogy reveals the presence of SD grains as the main carrier of remanent magnetization, paleointensity results are usually reliable. Where PSD and MD grains are the main carrier of remanent magnetization, the paleointensity

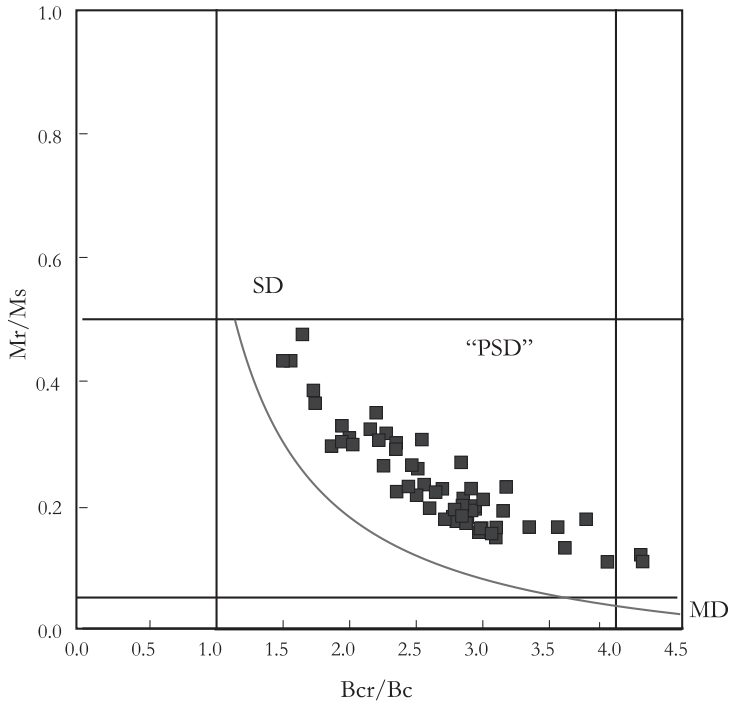

Fig. 2. Day plot (Day et al., 1977). SD, PSD, and MD refer to Single, Pseudo-single, and Multi domain behavior. The black squares are our data. The curved line represent the theoretical mixing SD MD equations of Dunlop (2002) using the constraints of Dunlop and Carter-Stiglitz (2006).

results are generally less ideal. Nonetheless, magnetic mineralogy from different sites sampled from the same flow, as well as different samples collected from the same site, display different mineralogical characteristics. Thus, we conclude that while mineralogical analyses might be useful for predicting which specimens will behave well during the paleointensity experiments, specimens from the same sample and samples from the same flows show different (magnetic) behaviors and the paleointensity experiment itself must provide the information necessary for accepting and rejecting specimen interpretations.

4.2. Paleointensity results

The results of the experiment are presented and analyzed through the 'Arai plots' (Nagata et al., 1963) in Fig. 3g–i and Fig. S1. We used the MagIC.py program (version pmagpy-2.214, http://earthref.org/PmagPy/cookbook) to process and display results of experiments. The results exhibit a variety of behaviors in the Arai plots. Three types of shapes have been observed in the Arai plots: 13.8% have a segmented or concave shape (Figs. 3i, S1 a, d), 8.3% have a zig-zagged character (Figs. 3i, S1h, i), and the remaining 77.9% exhibit straight or nearly straight lines (Figs. 3g and h and S1 b, c, e). Reliable paleointensity estimates have a linear Arai diagram, but specimens with nearly ideal behavior can depart slightly from linearity. The acceptability limits are still a matter of discussion. Despite the plethora of statistics to quantify the quality of the data, the selection of data remains subjective. To ensure the reliability of our interpretations, we have chosen rather strict selection criteria (see Paterson et al., 2014 and http://www.paleomag.net/SPD/home.html for definitions), which are listed in Table 2. For specimens passing our selection criteria (i.e. Grade A in Fig. 3g, h), the absolute value of the slope of the best-fit line (green lines in the diagrams) multiplied by the laboratory field yields the intensity of the ancient field (B in Fig. 3g, h, i). Specimens meeting our criteria (108 of 180) are listed in Supplement 2, representing a success rate of 60% at the specimen level. All of the data and interpretations have also been contributed to the MagIC database and can be accessed here: http://earthref.org/MagIC/9606. As suspected from phenomenological models and previous experimental results (e.g., Yu et al., 2004; Shaar et al., 2011), we confirm that the orientation of B_{TRM} and B_{NRM} can influence the degree of zig–zag (S1), which tends to disappear when B_{TRM} and B_{NRM} directions are nearly parallel. That said, when PSD or MD grains dominate, the behavior during the paleointensity experiment produces erratic or curved Arai plots and experiments fail, regardless of orientation. We suggest therefore that the effort of orienting specimens with respect to the laboratory field is not worthwhile, while pre-selecting specimens using their behavior during thermal demagnetization of the NRM (as suggested by Valet et al., 2010) may be (although variability among samples and specimens makes even this problematic). We find that those samples which show a rapid decrease of at least 70% of the initial magnetization over a narrow range of temperatures (close to Curie point), appear to perform better. Hysteresis statistics do not help during preselection, as there is no clear relation between the success of the experiments, most likely due to the non-uniqueness of hysteresis ratios in detecting domain state. Despite the carefulness in the pre-selection of suitable specimens, however, many specimens (~40%) still failed our selection criteria.

Specimens are taken as independent estimates of the field and are averaged at the lava flow level (Table 3). For this study we consider a site to be acceptable if at least 3 specimens with a standard deviation of at most 15% or 5 μT passed the selection criteria (Table 2). Nine sites failed as no reliable sample interpretations were found (Sml07, 10, 11, 16, 22, 24, 25, 30 and 33). The site level consistencies of the remaining sites (as indicated by σ) are between 0.9 and 11.6 μT (with an average of 4.7 μT) or between 1.9% and 14.3%. Paleointensity values range between ~38 μT (Queimado flow) and ~92 μT (Furna flow, radiocarbon dated to 593 ± 236 BC). Importantly, in most cases, sites from flows that are similar in age (e.g., Cascalho ~1300 AD, Ponta da Ferraria 1209 ± 54 AD, and Feteiras 1073 ± 90 AD) share similar paleointensity values (53.1 μT, 63.0 μT and 53.5 μT respectively). The two sites from the 1563 Queimado flow (Sml 19 and Sml 34) agree well

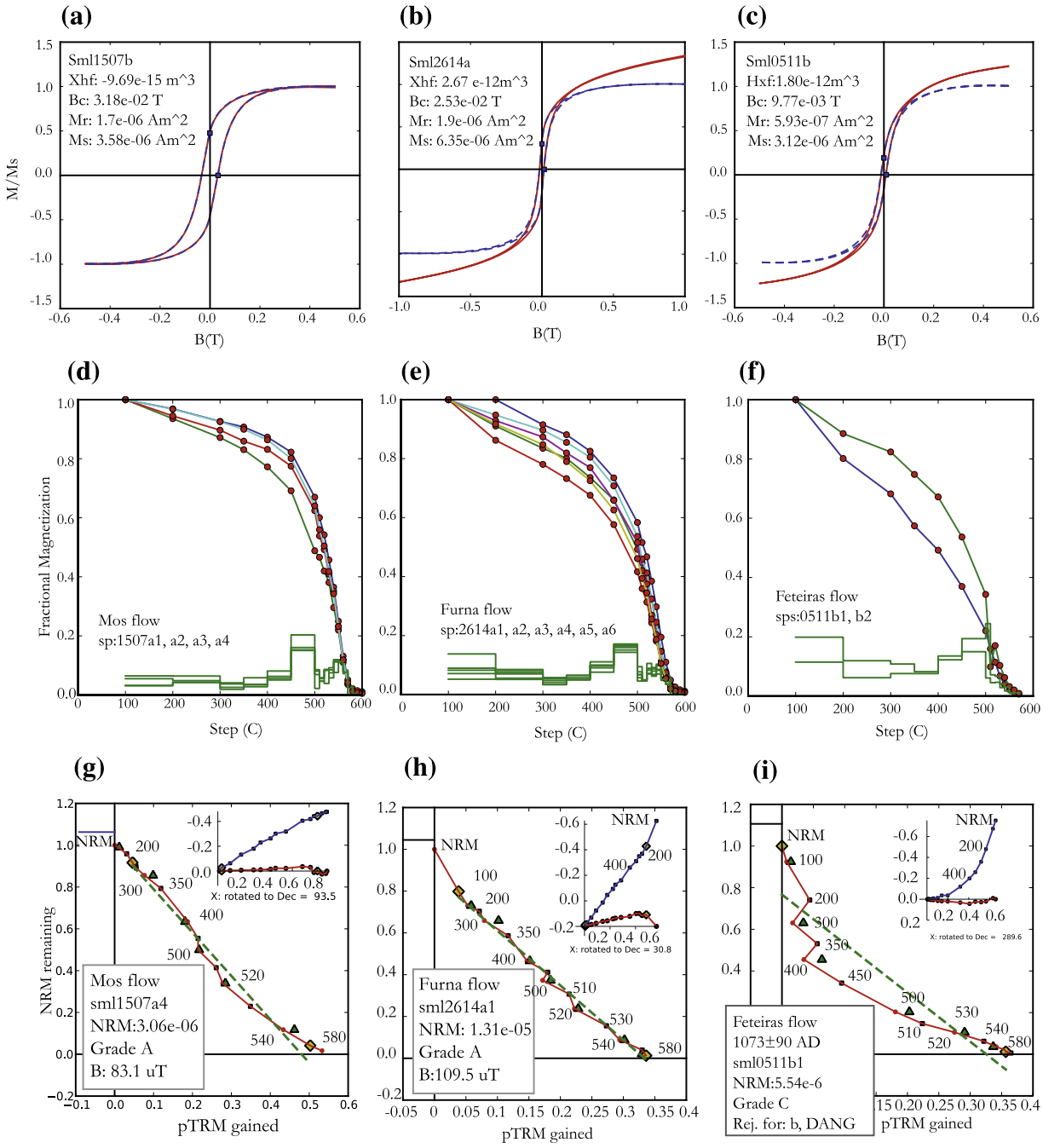

Fig. 3. Representative IZZI and hysteresis experimental results. (a–c) Hysteresis loops of sister specimens from three samples from different sites (a – from Mos flow; b – from Cruz N; and c – from Feteiras); blue dashed lines represent hysteresis loops corrected for the paramagnetic contribution (red continous lines uncorrected). (d–f) Fractional magnetization versus temperature of all the samples of the flows Mos, Furna, and Feteiras. (g–i) Arai plots and insets of Zijderveld diagrams of the specimens. The temperature interval used for isolating the characteristic remanence is marked with green dashed line and diamonds. The insets are the vector components of the zero field steps with x in the abscissa and y and *z* in the ordinate; the circles (red line) are (*x*, *y*) pairs and the squares (the temperature steps are marked alongside) are (*x*, *z*) pairs (blue line). The directions are in the specimen coordinate system. The laboratory field was 40 μT, applied along the *z*-axis in the in-field steps. (For interpretation of the references to colour in this figure legend, the reader is referred to the web version of this article.)

with one another (Table 2) and also with Sml 31 which was thought to represent the same eruption based on similarity in directions (Di Chiara et al., 2012). These three flows have been averaged together in Table 3.

5. Discussion

Fig. 4 is a summary of all directional (Di Chiara et al., 2012) and intensity (this study) results from the Azores as well as the vector components predicted for São Miguel (37.8°N, 25.5°W) by the most recent global field model, the CALS3k.4 by Korte and Constable (2011), the French archeomagnetic curve (Bucur, 1994; Gallet et al., 2002) and the ARCH3k.1 model of Korte et al. (2009). Our mean-paleointensity data vary from 38.5 ± 4.3 μT (Queimado flow) to 92.3 ± 11.6 μT (Furna flow). At first glance, our results agree with the global model predictions fairly well. Indeed, the maximum discrepancy between mean intensities and predictions from the Queimado flow (1563 AD), Feteiras (1073 ± 90 AD), Mata das Feiticeiras (1048 ± 113 AD), Caldeirão (675 ± 107 AD) and Ponta das Praias (240 ± 168 AD) flows is 9 μT. Considering that the

Table 3
Paleointensity results from sites and flows from São Miguel.

Flow name	Sites	Age (years ±)	σ (Age)	Dec (°)	Inc (°)	α_{95}	Intensity					
							N_B	B (μT)	σ	σ (%)	VADM	σ_{VADM}
Furna	Sml26;27	−593	236	13.0	58.0	2.7	17	92.3	11.6	12.5	163.5	20.5
Cruz N	Sml29	−750	250	8.7	57.5	2.6	7	55.7	8	14.3	98.8	14.1
Lagoa	Sml14	*~1500*	*200*	1.0	54.3	4.1	4	44.9	1.1	2.3	79.6	1.9
Ponta das Praias	Sml28	240	168	356.0	56.0	2.0	4	63.0	3.2	5.0	111.6	5.6
Caldeirão	Sml17	675	107	(−)	(−)	(−)	4	44.1	0.9	1.9	78.2	1.5
Caldeirão E	Sml23	675	107	12.6	57.3	4.6	3	54.5	3.5	6.5	96.6	6.3
Mos	Sml13;15	775	124	10.2	48.5	2.3	13	65.2	8.8	13.4	115.8	15.5
Mata das Feiticeiras	Sml21	1048	113	1.1	34.2	2.5	6	45.7	1.4	3.1	81.0	2.5
Feteiras	Sml01;02;03;05	1073	90	6.4	32.7	1.1	11	53.5	6.1	11.4	94.8	10.8
Ponta da Ferraria	Sml32	1209	54	355.4	32.4	2.4	5	60.0	2.1	3.5	106.2	3.7
Cascalho	Sml18	*~1300*	*0*	355.9	29.7	2.3	7	53.1	4.2	7.9	94.2	7.4
Queimado	Sml19;31;34	1563	0	0.5	55.5	1.5	11	38.5	4.3	11.1	68.2	7.6
Fogo 1x	Sml08	*~800*	*0*	11.1	47.7	2.3	8	78.0	5.9	7.6	138.4	10.5

Flow names and ages are defined as in Table 1. Ages in italic character are "paleomagnetically inferred", thus revised after combining paleodirections (Di Chiara et al., 2012) and intensity (this study). Declination and Inclination are from previous study. N is the number of specimens. Mean intensity results are reported by flow (μT and VADM converted), after IZZI experiments and processed using the "pmagpy-2.214" by L. Tauxe.

models are highly smoothed, the agreement is very good. However, the intensities from Furna, Caldeirão, Fogo and Lagoa are quite different from the expected values, using the ages assigned by Di Chiara et al. (2012).

Ten of the studied flows are radiocarbon dated by Moore (1990) and Moore and Rubin (1991). Three lava flows had been archaeomagnetically dated by Di Chiara et al. (2012): Cruz N (Sml29; 400–700 BC), Cruz S (Sml11; 0–200 AD), and Lagoa (Sml14; 100–400 AD). Taking our new paleointensity results into account, we validate or re-assess some of these paleomagnetic ages. Unfortunately, Cruz S did not pass our selection critera; Cruz N agrees with the predicted intensity value within error, while the intensity from Lagoa deviates from the expected values by about 15 μT. We suggest that either the field was lower than predicted by the global model, or the paleomagnetic directions in some cases are not sufficient for dating and the inferred ages of the site were erroneously assigned. Stressing that there were few data points in the Atlantic Ocean region to constrain the global model, we nonetheless observe that predicted directional values agree reasonably well with the data of Di Chiara et al., 2012, particularly the ARCH3k model. Additionally, the direction of the Ponta das Praias flow (Sml28, ~240 AD), is in good agreement with the models, and has an intensity significantly higher than the Lagoa site. Thus, we suggest that the age of Lagoa estimated using paleomagnetic directions (which can be non-unique) was erroneously assigned and reconsider the age here.

Considering paleodirection (Declination, D, and Inclination, I, Table 2) and paleointensity values and comparing them with the CALS3k.4 (from 0 to 3 ka), CALS10k (from 3 to 10 ka, by Korte et al., 2011), and ARCH3k.1 (from 0 to 3 ka), we find that the Lagoa flow is in fact not uniquely dated by the field models. Effectively, the low values of declination (1.0°), inclination (54.3°) and intensity (44.9 μT) of Lagoa flow are comparable with the minimum reported in the CALS10k (Korte et al., 2011) in D, I and intensity (359.7°, 52.0° and 40.8 μT, respectively) at around 3100 BC. Another possibility is that the site Sml14 of the Lagoa flow could even be historical (1400 ± 200 AD), since it was sampled in a lava flow between two branches of the 1652 AD Fogo flow (according to the geological map of Moore, 1990). We infer that this second hypothesis is the most likely, as the 1563 AD Queimado flow yielded similar values (D = 0.5°, I = 55.5° and intensity = 38.5 μT).

The historical flow Fogo is characterized by an inclination (47.7°), which is discrepant with respect to the global models (e.g., GUFM1 predicted an inclination of 63°), raising the suspicion that either a rapid inclination drop occurred 150 years before the GUFM1 prediction in the Atlantic area, or some problem in recording the paleomagnetic field occurred in the flow, or the paleomagnetic sites were erroneously mapped as the Fogo flow but belong instead to a slightly older flow. While the directions of Sml08 and Sml10 are consistent with each other, we cannot test the intensities of Sml10 as it failed our seletion criteria. Therefore we suggest that Sml08 (named here Fogo 1x) is somewhat older than reported, and both direction and intensity suggest that it could have been erupted at ~800 AD (similar to the Sml13).

The age of the Cascalho flow (Sml18) was constrained using stratigraphic evidence and paleomagnetic directions. Indeed it was initially thought to fall in the 1300–1500 AD time window. However, the inclinations are much lower than the Queimado flow of 1563 AD (Sml19, 31 and 34) all of which are consistent with the model predictions. Therefore, we reassign it to have an age within the lower bound of the interval (~1300 AD). The intensity of 53.1 ± 4.2 μT supports this hypothesis as the intensity agrees well with those obtained for the 1000–1300 AD age interval (~55 μT), whereas it is significantly different from the values of Queimado (38.5 ± 4.3 μT).

Paleomagnetic directions from the Caldeirão flow (Sml17) agree well with global model predictions, especially with the ARCH3k.1. The paleointensity of Sml23 (here named Caldeirão E) is 10 μT lower than Sml17.

5.1. Paleointensities over the last 3 ka

We have calculated mean values of paleomagnetic intensities and converted them to virtual axial dipole moments (VADM, e.g. Tauxe, 2009). These are listed in Table 3 and plotted in Fig. 5; those with revised ages are indicated by the open, dashed symbols. We also show data from Morocco (Kovacheva, 1984; Gómez-Paccard et al., 2012), Portugal (Nachasova and Burakov, 2009 and Hartmann et al., 2009), Spain (Gómez-Paccard et al., 2006, 2008, 2012; Nachasova et al., 2007; Catanzariti et al., 2012; Beamud et al., 2012), and France (Chauvin et al., 2000; Genevey and Gallet 2002; Gallet et al., 2003; Genevey et al., 2009; Gómez-Paccard et al., 2012). The regional curve has two maxima (around 600–800 AD and 600–400 BC, separated by a minimum at around 0–500 AD. The 600–400 BC maximum is well reproduced by our Furna flow (593 ± 236 BC) reaching a high of 92.3 μT (163.5 ± 20.5 ZAm^2). This result is robust as it is based on an average of 17 specimens from two flows (sampled 3 km apart from each other) belonging to the same volcanic event. Similar high field values around the same time interval are observed in the Western

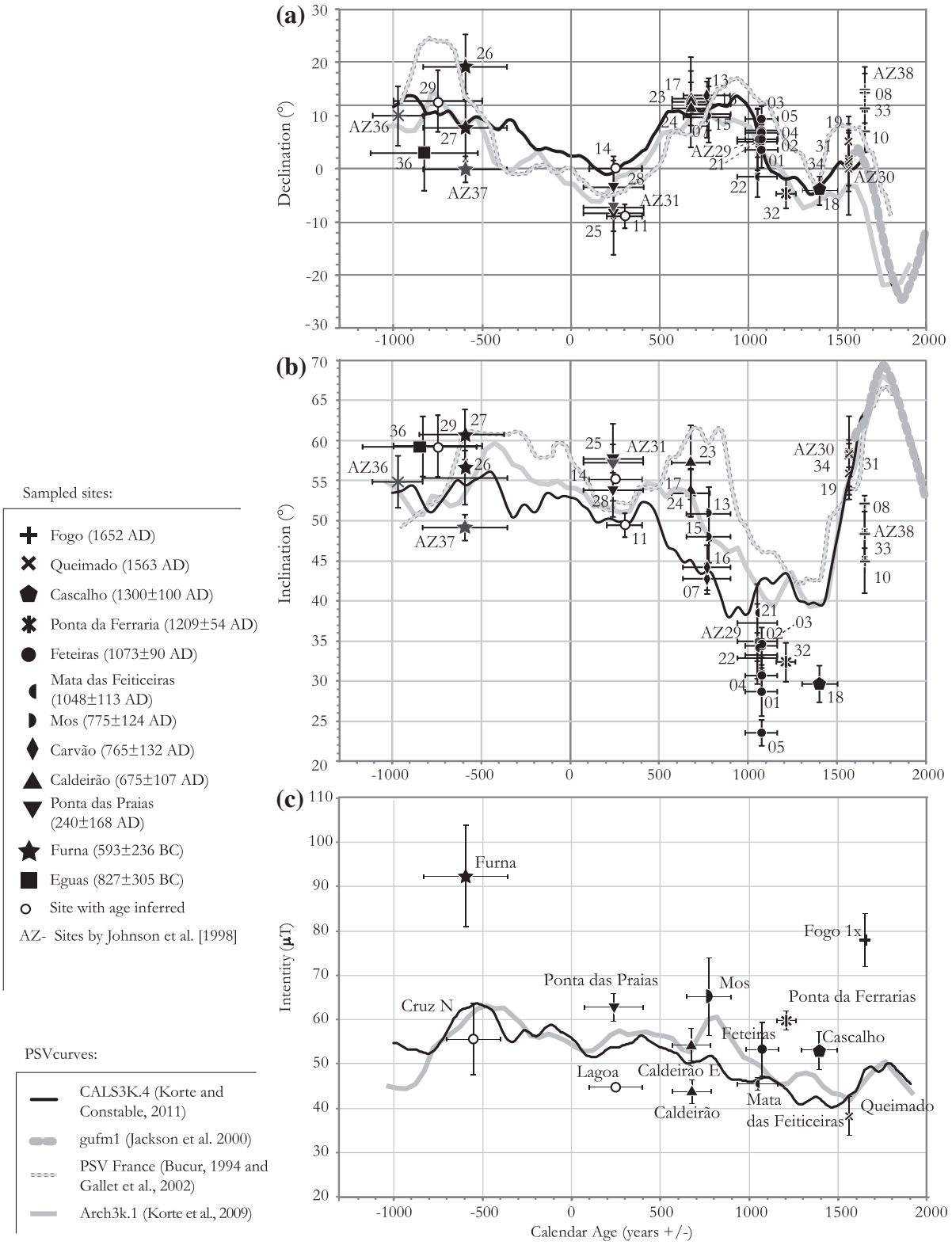

Fig. 4. (a) Declination and (b) inclination of paleomagnetic directions previously recovered by Di Chiara et al. (2012), versus age for historical and ^{14}C dated site mean directions. In (a) and (b) declination/inclination pairs are compared with global field model predictions from GUFM (Jackson et al., 2000), CALS3 k.4 (Korte and Constable, 2011), ARCH3k.1 (Korte et al., 2009) and the French curve (Bucur, 1994; Gallet et al., 2002). (c) Mean intensities obtained from each flow (this study). Ages are calendar ages calibrated from ^{14}C ages reported by Moore and Rubin (1991) using CALIB6.0 (http://calib.qub.ac.uk/calib/calib.html).

USA (Champion, 1980) with values up to 140 ZAm^2, and even higher values of 197.5 ZAm^2 from Hawaii (Pressling et al., 2006) around 840 BC. The high value recovered on the Hawaiian samples was not reproduced after a re-measurement of the samples however (Pressling et al., 2007). A regional spike was also recorded in Europe (Genevey et al., 2003; Gallet et al., 2006; Gallet and Le

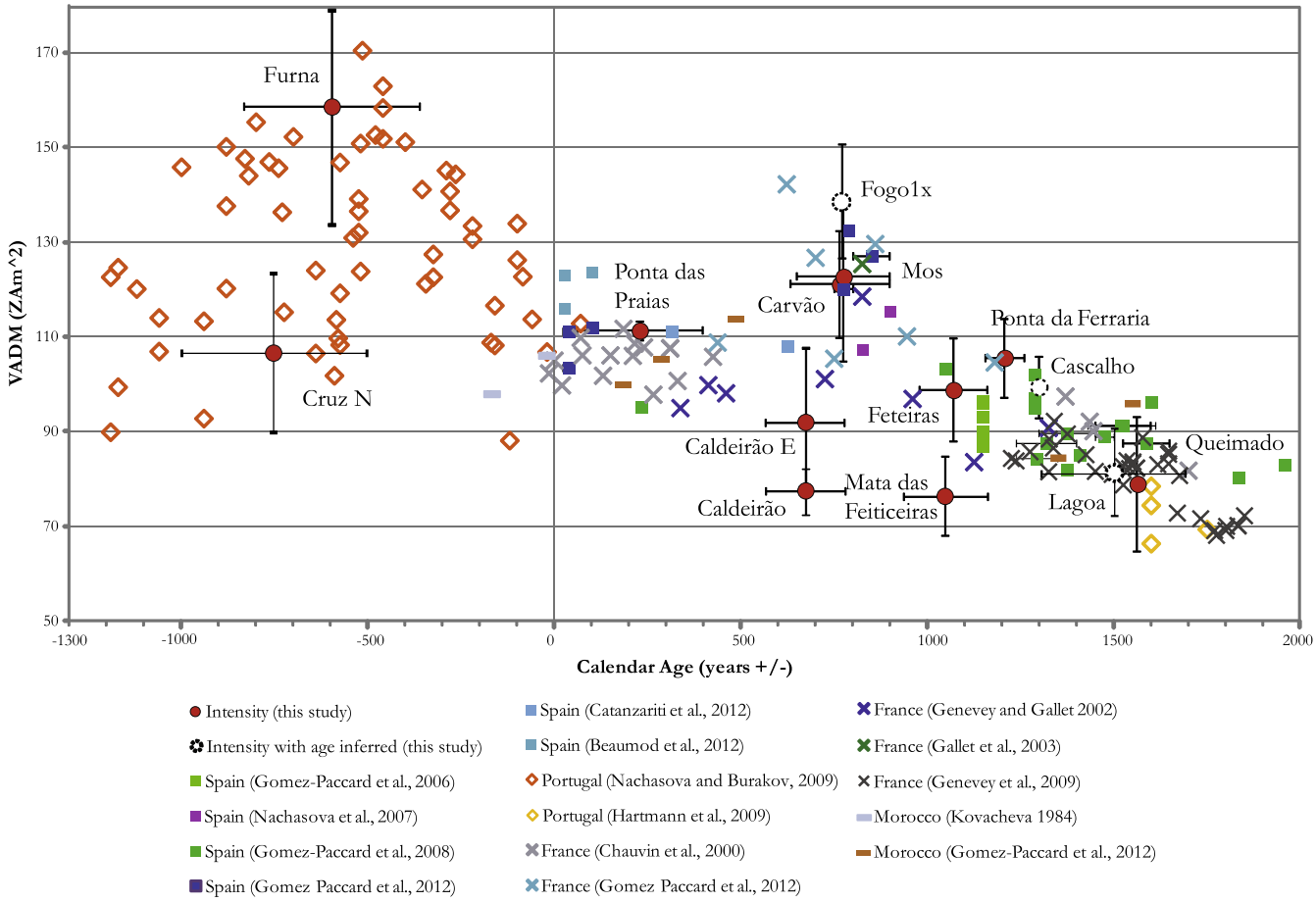

Fig. 5. Paleointensity flow means are compared with data from Morocco (Kovacheva, 1984 and Gómez-Paccard et al., 2012) and Europe: Portugal (Nachasova and Burakov, 2009 and Hartmann et al., 2009), Spain (Gómez-Paccard et al., 2006, 2008, 2012; Nachasova et al., 2007; Catanzariti et al., 2012; Beamud et al., 2012), and France (Chauvin et al., 2000; Genevey and Gallet, 2002; Gallet et al., 2003; Genevey et al., 2009; Gómez-Paccard et al., 2012). The ages of Lagoa, Cascalho, Fogo1x and Cruz N flows were reassigned according to the new intensity results.

Goff, 2006), in Syria (Genevey et al., 2003) and in Southern Jordan (reaching as high as 213 ZAm^2, Ben-Yosef et al., 2008, 2009) at around 800 and 1000 BC respectively. However, there is a discrepancy between the Levantine curve and the Grecian master curve (De Marco et al., 2008), which highlights a peak of intensity of 114 ZAm^2 around ~600–500 BC. Regardless of the age difference of the peak in intensity and the irregular distribution of datasets, both European and Azorean data suggest the possibility of a large scale intensity high, and encourage further investigation of the regional extent of this feature. Recent data from Eastern Asia by Cai et al. (2014) argue against the global nature of this feature because they do not find any peak of intensity around ~1000 BC in China, suggesting that it may not be global; rather, the peaks in the Levantine and Southern European curves are distinct features of the non-dipole field. Interestingly, the archeomagnetic data of Hong et al. (2013) from South Korea display strong values of field intensity of 130 ZAm^2 at around ~1300 BC, explained either as a result of the migration of persistent flux in the northern hemisphere or as an episode of geomagnetic field hemispheric asymmetry.

Interesting insights result from the comparison of our dataset and the data provided by Mitra et al. (2013): seventeen archeointensity estimates from Senegal and Mali (West Africa) covering a time period between 1000 BC and 1000 AD. These data were compared with data from Morocco and Egypt, and also with European data, dividing data into three latitudinal intervals: 0°–20°, 20°–40° and 40°–60° N. They found a strong latitudinal gradient in VADM values, especially in the time range between 100 and 1000 AD, whereas from 0 to 1000 BC data from both 20°–40° and 40°–60° reproduce a prominent feature culminating around 600 BC with a maximum (up to 120 ZAm^2). The latitudinal gradient is explained as changing non-axial-dipole contributions represented by the simulation at the core mantle boundary using the CALS3k.4 model (Korte and Constable, 2011), whereas the structure of the field around 0–100 AD was more axial-dipolar. Our data (at a latitude of 38°N) support the conclusion of Mitra et al. (2013) for the age interval between 400 and 1200 AD, whereas our values are even higher than those in the compilation of Mitra et al. (2013), especially for the peak of high intensity around 600 BC.

6. Conclusion

New paleointensity data from lava flows many of which have excellent age control from the last 3000 years (Moore, 1990, 1991; and Moore and Rubin, 1991) are presented in this study. All the samples previously investigated to recover paleodirections have been subjected to a strict pre-selection process in order to choose the most suitable samples for paleointensity experiments.

We obtained 20 new paleointensity estimates from 13 lava flows. Ten lava flows were radiocarbon dated, whereas three flows were dated by Di Chiara et al. (2012); one site was dated using stratigraphic relations. The paleomagnetically dated flows (Cruz N, and Lagoa) have mean flow intensities that are different from

those predicted and we revise their ages; Cruz N is slightly older, and Lagoa could be younger or older (~1500 AD or ~3100 BC) than previously stated. The CALS10k.1b model (Korte et al., 2011) predicts declinations of −3°, inclination of 52° and intensity of 39 μT around 3400 BC. There are other times when the field was low according to the model before 3000 BC (inclination and declination also), and so the dating is not certain. The age of the Cascalho flow around 1,300 AD is confirmed by the paleointensity.

The intensity of the site Sml08 assigned to the 1652 AD historical flow of Fogo 1 is particularly high (78.0 μT). Since the direction is also different from the expected values for this age, we suggest that the flow sampled at Sml08 may be older.

The peak of intensity up to ~ 90 μT around 600 BC is well supported by two sites from the same flow (Furna). It is noteworthy that our results are comparable to the "spike" of intensity in the Levantine records, as well as in Western Europe.

Our data confirm the conclusion of Mitra et al. (2013) of a predominance of the axial-dipole component between 0 to 100 AD, and a strong latitudinal gradient from 100 to 1000 AD. The maximum in field values around 500–600 BC is well reproduced and even enhanced.

We conclude that:

- Paleomagnetic dating requires the three components of the geomagnetic field (declination, inclination and intensity) and a well determined global model (see Lanos, 2004).
- Since some of the studied flows diverge from the predicted paleomagnetic behavior either some of the conclusions in the earlier paper are inconsistent, or some of the flows mapped by Moore (1990) may be multiple flows so the geological map needs to be improved.
- Our data are consistent with the conclusions of Mitra et al. (2013) that there is a high latitudinal gradient in the field at 500–600 BC, and at 0 AD, our data require no field gradient. Around 800 AD, the gradient appears again.
- Our data represent the first dataset of reliable paleointensity estimates for the central-northern Atlantic Ocean. The new data are internally consistent and radiocarbon dated, so they can be included in global geomagnetic datasets, and safely used to enhance the next global model of the geomagnetic field.

Acknowledgements

A.D.C. thanks Jason Steindorf for laboratory support, R. Mitra for useful discussions and helpfulness, acknowledges a Marco Polo grant from the Bologna University, and thanks the FAPESP support (2013/08938-8). A.D.C. and F.S. were funded by INGV and FIRB MIUR C2 funds (responsible L. Sagnotti). This research was partially supported by National Science Foundation grant EAR1141840 to L. T.

Appendix A. Supplementary data

Supplementary data associated with this article can be found, in the online version, at http://dx.doi.org/10.1016/j.pepi.2014.06.008.

References

Abdel-Monem, A.A., Fernandez, L.A., Boone, G.M., 1975. K–Ar ages from the eastern Azores group (Santa Maria, São Miguel and the Formigas Islands). Lithos 8 (4), 247–254. http://dx.doi.org/10.1016/0024-4937(75) 90008-0.

Abokodair, A.A., 1977. The Accuracy of the Thelliers' Technique for the Determination of Paleointensities of the Earth's Magnetic Field., PhD Thesis, University of California, Santa Cruz.

Aitken, M.J., Allsop, A.L., Bussell, G.D., Winter, M.B., 1988. Determination of the intensity of the Earth's magnetic field during archaeological times: reliability of the Thellier technique. Rev. Geophs. 26 (1), 3–12.

Beamud, E., Gómez-Paccard, M., McIntosh, G., Larrasoaña, J.C., 2012. New archaeomagnetic data from three roman kilns in northeast Spain: a contribution to the Iberian palaeosecular variation curve. Geophys. Res. Abstr., 14, EGU2012-8232.

Ben-Yosef, E., Tauxe, L., Ron, H., Agnon, A., Avner, A., Najjar, M., Levy, T.E., 2008. A new approach for geomagnetic archaeointensity research: insights on ancient metallurgy in the Southern Levant. J. Archaeol. Sci. 35, 2863–2879.

Ben-Yosef, E., Tauxe, L., Levy, T.E., Shaar, R., Ron, R., Najjar, M., 2009. Geomagnetic intensity spike recorded in high resolution slag deposit in Southern Jordan. Earth Planet. Sci. Lett. 287, 529–539. http://dx.doi.org/10.1016/j.epsl.2009.09.001.

Biggin, A.J., 2006. First-order symmetry of weak-field partial thermoremanence in multi-domain (MD) ferromagnetic grains. 2. Implications for Thellier-type palaeointensity determination. Earth Planet. Sci. Lett. 245, 454–470.

Biggin, A.J., 2010. Are systematic differences between thermal and microwave Thellier-type palaeointensity estimates a consequence of multidomain bias in the thermal results? Phys. Earth Planet. Inter. 180, 16–40.

Biggin, A.J., Poidras, T., 2006. First-order symmetry of weak-field partial thermoremanence in multi-domain ferromagnetic grains. 1. Experimental evidence and physical implications. Earth Planet. Sci. Lett. 245, 438–453.

Biggin, A.J., Thomas, D.N., 2003. Analysis of long-term variations in the geomagnetic poloidal field intensity and evaluation of their relationship with global geodynamics. Geophys. J. Int. 152 (2), 392–415.

Booth, B., Croasdale, R., Walker, G.P.L., 1978. A quantitative study of five thousand years of volcanism on São Miguel, Azores. Philos. Trans. R. Soc. London A. 288, 271–319. http://dx.doi.org/10.1098/rsta.1978.0018.

Bowles J., Gee J.S., Kent D., Bergmanis, E., Sinton, J., 2005. Cooling rate effects on paleointensity estimates in submarine basaltic glass and implications for dating young flows. Geochem. Geophys. Geosyst. 6. doi:10.1029/2004GC000900.

Bucur, I., 1994. The direction of the terrestrial magnetic field in France during the last 21 centuries. Recent progress. Phys. Earth Planet. Inter. 87, 95–109. http://dx.doi.org/10.1016/0031-9201(94)90024-8.

Cai, S., Tauxe, L., Deng, C., Pan, Y., Jin, G., Zheng, J., Xie, F., Qin, H., Zhu, R., 2014. Geomagnetic intensity variations for the past 8 kyr: New archaeointensity results from Eastern China. Earth Planet. Sci. Lett. 392, 217–229.

Calvo, M., Prèvot, M., Perrin, M., Riisager, J., 2002. Investigating the reasons for the failure of palaeointensity experiments: a study on historical lava flows from Mt. Etna (Italy). Geophys. J. Int. 149, 44–63.

Carlut, J., Kent, D.V., 2000. Paleointensity record in zero-age submarine basalt glasses: testing a new dating technique for recent MORBs. Earth Planet. Sci. Lett. 183, 389–401.

Carlut, J., Cormier, M.H., Kent, D.V., Donnelly, K.E., Langmuir, C.H., 2004. Timing of volcanism along the northern East Pacific Rise based on paleointensity experiments on basaltic glasses. J. Geophys. Res. 109, B04104.

Catanzariti, G., Gòmez-Paccard, M., McIntosh, G., Pavòn-Carrasco, F.J., Chauvin, A., Osete, M.L., 2012. New archaeomagnetic data recovered from the study of Roman and Visigothic remains from central Spain (3rd–7th centuries). Geophys. J. Int. http://dx.doi.org/10.1111/j.1365-246X.2011.05315.x.

Champion, D.E., 1980. Holocene Geomagnetic Secular Variation in the Western United States: Implications for the Global Geomagnetic Field, Dissertation (Ph.D.), California Institute of Technology.

Chauvin, A., Garcia, Y., Lanos, Ph., Laubenheimer, F., 2000. Paleointensity of the geomagnetic field recovered on archaeomagnetic sites from France. Phys. Earth Planet. Inter. 120, 111–136.

Chauvin, A., Roperch, P., Levi, S., 2005. Reliability of geomagnetic paleointensity data: the effects of the NRM fraction and concave up behaviour on paleointensity determination by Thellier method. Phys. Earth Planet. Inter. 150, 265–286.

Coe, R.S., 1967. The determination of paleo-intensities of the Earth's magnetic field with emphasis on mechanisms which could cause non-ideal behavior in Thellier's method. J. Geomagn. Geoelectric. 19, 157–179.

Coe, R.S., Gromme, S., Manknen, E.A., 1978. Geomagnetic paleointensities from radiocarbon-dated lava flows on Hawaii and the question of the Pacific nondipole low. J. Geophys. Res. 83, 1740–1756.

Coe, R.S., Riisager, J., Plenier, G., Leonhardt, R., Kràs, D., 2004. Multidomain behavior during Thellier paleointensity experiments: results from the 1915 Mt. Lassen flow. Phys. Earth Planet. Inter. 147, 141–153.

Cromwell, G., Tauxe, L., Staudigel, H., Ron, H., Trusdell, F., 2011. Paleointensity results for 0 and 3 ka from Hawaiian lava flows: a new approach to sampling. American Geophysical Union. Fall Meeting 2011, abstract #GP13A-08.

Cromwell, G, Tauxe, L., Staudigel, H., Ron, H., Trusdell, F., 2012. Paleointensity results for 0 and 4 ka from Hawaiin lava flows: a new approach to sampling. EGU General Assembly. Geophys. Res. Abstr. 14, EGU2012-01608.

Day, R., Fuller, M., Schmidt, V.A., 1977. Hysteresis properties of titanomagnetites: grain-size and compositional dependence. Phys. Earth Planet. Inter. 13, 260–267.

De Marco, E., Spatharas, V., Gómez-Paccard, M., Chauvin, A., Kondopoulou, D., 2008. New archaeointensity results from archaeological sites and variation of the geomagnetic field intensity for the last 7 millennia in Greece. Phys. Chem. Earth 33, 578–595.

DeGroot, L.V., Biggin, A.J., Dekkers, M.J., Langereis, C., Herrero-Bervera, H., 2013. Rapid regional perturbations to the recent global geomagnetic decay revealed by a new Hawaiian record. In: Nat. Commun 4, 2727. http://dx.doi.org/10.1038/ncomms3727.

Dekkers, M.J., Boehnel, H.N., 2006. Reliable absolute palaeointensities independent of magnetic domain state. Earth Planet. Sci. Lett. 248, 508–517.

Di Chiara, A., Speranza, F., Porreca, M., 2012. Paleomagnetic secular variation at the Azores during the last 3 ka. J. Geophys. Res. 117, B07101. http://dx.doi.org/10.1029/2012JB009285.
Donadini, F., Korhonen, K., Riisager, P., Pesonen, L.J., 2006. Database for Holocene geomagnetic intensity information. EOS Trans. Am. Geophys. Union 87 (14), 137.
Donadini, F., Korte, M., Constable, C.G., 2009. Geomagnetic field for 0–3 ka: 1. New data sets for global modeling. Geochem. Geophys. Geosyst. 10, Q06007. http://dx.doi.org/10.1029/2008GC002295.
Dunlop, D.J., 2002. Theory and application of the Day plot (Mrs/Ms versus Hcr/Hc) 1. Theoretical curves and tests using titanomagnetite data, J. Geoph. Res. 107 (B3). DOI: 10.1029/2001JB000486.
Dunlop, D.J., Carter-Stiglitz, B., 2006. Day plots of mixtures of superparamagnetic, single-domain, pseudosingledomain, and multidomain magnetites, J. Geophys. Res. 111, B12S09. doi:10.1029/2006JB004499.
Fabian, K., 2001. A theoretical treatment of paleointensity determination experiments on rocks containing pseudo-single or multi domain magnetic particles. Earth Planet. Sci. Lett. 188, 45–58.
Feraud, G., Kaneoka, I., Allègre, C.J., 1980. K/Ar ages and stress pattern in the Azores: geodynamic implications. Earth Planet. Sci. Lett. 46, 275–286. http://dx.doi.org/10.1016/0012-821X(80)90013-8.
Ferk A., Leonardht, R., Richard, D., Aulock, F., Hess, K., Dingwell, D., 2008. Paleointensity study on subaerial volcanic glass. Geophys. Res. Abstr. 10, EGU2008-A-06936.
Gallet, Y., Le Goff, M., 2006. High-temperature archeointensity measurements from Mesopotamia. Earth Planet. Sci. Lett. 241, 159–173.
Gallet, Y., Genevey, A., Le Goff, M., 2002. Three millennia of directional variation of the Earth's magnetic field in western Europe as revealed by archaeological artefacts. Phys. Earth Planet. Inter. 131, 81–89. http://dx.doi.org/10.1016/S0031-9201(02)00030-4.
Gallet, Y., Genevey, A., Courtillot, V., 2003. On the possible occurrence of archeomagnetic jerks in the geomagnetic field over the past three millennia. Earth Planet. Sci. Lett. 214, 237–242.
Gallet, Y., Genevey, A., Le Goff, M., Fluteau, F., Eshraghi, S.A., 2006. Possible impact of the Earth's magnetic field on the history of ancient civilizations. Earth Planet. Sci. Lett. 246, 17–26.
Garcia, A.S., Thomas, D.N., Liss, D., Shaw, J., 2006. Low geomagnetic field intensity during the Kiaman superchron: thellier and microwave results from the Great Whin Sill intrusive complex, northern United Kingdom. Geophys. Res. Lett. 33 (16). http://dx.doi.org/10.1029/2006GL026729.
Gee, J.S., Cande, S.C., Hildebrand, J.A., Donnelly, K., Parker, R.L., 2000. Geomagnetic intensity variations over the past 780 kyr obtained from near-seafloor magnetic anomalies. Nature 408, 827–832.
Genevey, A., Gallet, Y., 2002. Intensity of the geomagnetic field inwestern Europe over the past 2000 years: new data from ancient French potteries. J. Geophys. Res. 107. http://dx.doi.org/10.1029/2001JB000701.
Genevey, A., Gallet, Y., Margueron, J.-C., 2003. Eight thousand years of geomagnetic field intensity variations in the eastern Mediterranean. J. Geophys. Res. 108. http://dx.doi.org/10.1029/2001JB001612.
Genevey, A., Gallet, Y., Constable, C.G., Korte, M., Hulot, G., 2008. ArcheoInt: an upgraded compilation of geomagnetic field intensity data for the past ten millennia and its application to the recovery of the past dipole moment. Geochem. Geophys. Geosyst. 9 (4), Q04038. http://dx.doi.org/10.1029/2007GC001881.
Genevey, A., Gallet, Y., Rosen, J., Le Goff, M., 2009. Evidence for rapid geomagnetic field intensity variations in Western Europe over the past 800 years from new French archaeointensity data. Earth Plant. Sci. Lett. 284, 132–143.
Gómez-Paccard, M., Chauvin, A., Lanos, P., McIntosh, G., Osete, M.L., Catanzariti, G., Ruiz-Martínez, V.C., Núñez, J.I., 2006. First archaeomagnetic secular variation curve for the Iberian Peninsula: comparison with other data from western Europe and with global geomagnetic field models. Geochem. Geophys. Geosyst. 7, Q12001. http://dx.doi.org/10.1029/2006GC001476.
Gómez-Paccard, M., Chauvin, A., Lanos, P., Thiriot, J., 2008. New archeointensity data from Spain and the geomagnetic dipole moment in western Europe over the past 2000 years. J. Geophys. Res. 113, B09103. http://dx.doi.org/10.1029/2008JB005582.
Gómez-Paccard, M., McIntosh, G., Chauvin, A., Beamud, E., Pavòn-Carrasco, F.J., Thiriot, J., 2012. Archaeomagnetic and rock magnetic study of six kilns from North Africa (Tunisia and Morocco). Geophys. J. Int. 189, 169–186. http://dx.doi.org/10.1111/j.1365-246X.2011.05335.x.
Granot, R., Tauxe, L., Gee, J.S., Ron, H., 2006. A view into the Cretaceous geomagnetic field from analysis of gabbros and submarine glasses. Earth Planet. Sci. Lett. 256 (1–2), 1–11.
Hagstrum, J.T., Champion, D.E., 1994. Paleomagnetic correlation of Late Quaternary lava flows in the lowest east rift zone of Kilauea Volcano, Hawaii. J. Geophs. Res. 99 (B11), 21679–21690.
Hartmann, G.A., Trindade, R.I.F., Goguitchaichvili, A., Etchevarne, C., Morales, J., aAfonso, M.C., 2009. First archeointensity results from Portuguese potteries (1550–1750 AD). Earth Planets Space 61, 93–100.
Herrero-Bervera, E., Valet, J.P., 2009. Testing determinations of absolute paleointensity from the 1955 and 1960 Hawaiian flows. Earth Planet. Sci. Lett. 287, 420–433.
Hill, M.J., Shaw, J., 2000. Magnetic field intensity study of the 1960 Kilauea lava flow, Hawaii, using the microwave palaeointensity technique. Geophys. J. Int. 142, 487–504.
Hoffman, K.A., Constantine, V.L., Morse, D.L., 1989. Determination of absolute paleointensity using a multi-specimen procedure. Nature 339, 295–297.
Hong, H., Yu, Y., Hee Lee, C., Kim, R.H., Park, J., Doh, S.J., Kim, W., Sung, J., 2013. Globally strong geomagnetic field intensity circa 3000 years ago. Earth Planet. Sci. Lett. 383, 142–152.
Jackson, A., Jonkers, A.R.T., Walker, M.R., 2000. Four centuries of geomagnetic secular variation from historical records. R. Soc. London Philos. Trans. 358, 957–990.
Johnson, C.L., Wijbrans, J.R., Constable, C.G., Gee, J., Staudigel, H., Tauxe, L., Forjaz, V.H., Salgueiro, M., 1998. $^{40}Ar/^{39}Ar$ ages and paleomagnetism of São Miguel lavas, Azores. Earth Planet. Sci. Lett. 160, 637–649.
Kissel, C., Laj, C., 2004. Improvements in procedure and paleointensity selection criteria (PICRIT-03) for Thellier and Thellier determinations: application to Hawaiian basaltic long cores. Phys. Earth Planet. Inter. 147, 155–169.
Korte, M., Constable, C.G., 2011. Improving geomagnetic field reconstruction for 0–3 ka. Phys. Earth Planet. Inter. 188, 247–259. http://dx.doi.org/10.1016/j.pepi.2011.06.017.
Korte, M., Donadini, F., Constable, C.G., 2009. Geomagnetic field for 0–3 ka: 2. A new series of time-varying global models. Geochem. Geophys. Geosyst. 10, Q06008. http://dx.doi.org/10.1029/2008GC002297.
Korte, M., Constable, C.G., Donadini, F., Holme, R., 2011. Reconstructing the Holocene geomagnetic field. Earth Planet. Sci. Lett. 312 (3–4), 497–505.
Kovacheva, M., 1984. Some archaeomagnetic conclusions from three archaeological localities in North-West Africa, Comptes Rendus de l'Acad. Bulgare des Sci. 3712, 171–174.
Lanos, P., 2004. Bayesian inference of calibration curves: application to archaeomagnetism. In: Buck, C., Millard, A. (Eds.), Tools for Constructing Chronologies: Crossing Disciplinary Boundaries, vol. 177, Springer-Verlag, London, pp. 43–82.
Leonhardt, R., Kràsa, D., Coe, R.S., 2004. Multidomain behavior during Thellier paleointensity experiments: a phenomenological model. Phys. Earth Planet. Inter. 147, 127–140.
Levi, S., 1977. The effect of Magnetite particle size on paleointensity determinations of the geomagnetic field. Phys. Earth Planet. Inter. 13, 245–259.
McClelland, E., Briden, J.C., 1996. An improved methodology for Thellier-type paleointensity determination in igneous rocks and its usefulness for verifying primary thermoremanence. J. Geophys. Res. 101, 21995–22013.
Michalk, D.M., Muxworthy, A.R., Böhnel, H.N., Maclennan, J., Nowaczyk, J.N., 2008. Evaluation of the multispecimen parallel differential pTRM method: a test on historical lavas from Iceland and Mexico. Geophys. J. Int. 173, 409–420.
Mitchell-Thomè, R.C., 1981. Vulcanicity of historic times in the Middle Atlantic Islands. Bull. Volcanol. 44, 57–69.
Mitra, R., Tauxe, L., Mcintosh, S.K., 2013. Two thousand years of archeointensity from West Africa. Earth Planet. Sci. Lett. 364, 123–133.
Moore, R.B., 1990. Volcanic geology and eruption frequency, São Miguel, Azores. Bull. Volcanol. 52, 602–614. http://dx.doi.org/10.1007/BF00301211.
Moore, R.B., 1991. Geologic map of São Miguel, Azores, U.S. Geol. Surv. Misc. Invest. Map, I-2007, scale 1:50,000.
Moore, R.B., Rubin, M., 1991. Radiocarbon dates for lava flows and pyroclastic deposits on São Miguel, Azores. Radiocarbon 33 (1), 151–164.
Nachasova, I.E., Burakov, K.S., 2009. Variation of the intensity of the Earth's magnetic field in Portugal in the 1st Millennium BC. Phys. Solid Earth 45 (7), 595–603.
Nachasova, I.E., Burakov, K.S., Molina, F., Cámara, J.A., 2007. Archaeomagnetic study of ceramics from the Neolithic Los Castillejos multilayer monument (Montefrio, Spain), Izvestiya. Phys. Solid Earth 43 (2), 170–176.
Nagata, T., Arai, Y., Momose, K., 1963. Secular variation of the geomagnetic total force during the last 5000 years. J. Geophys. Res. 68, 5277–5281.
Pan, Y., Shaw, J., Zhu, R., Hill, M.J., 2002. Experimental reassessment of the Shaw paleointensity method using laboratory-induced thermal remanent magnetization. J. Geophys. Res. B 107, 2002. http://dx.doi.org/10.1029/2001JB000620 (B7).
Paterson, G.A., Biggin, A.J., Yamamoto, Y., Pan, Y., 2012. Towards the robust selection of Thellier-type paleointensity data: the influence of experimental noise. Geochem. Geophs. Geosyst. 13(5), Q05Z43. doi:10.1029/2012GC004046.
Paterson, G.A.L., Tauxe, A.J. Biggin, R. Shaar, Jonestrask, L.C., 2014. On improving the selection of Thellier-type paleointensity data. Geochem. Geophys. Geosyst. doi: 10.1002/2013GC005135.
Pavón-Carrasco, F.J., Osete, M.L., Torta, J.M., De Santis, A., 2014. A geomagnetic field model for the Holocene based on archaeomagnetic and lava flow data. Earth Planet. Sci. Lett. 388, 98–109.
Pick, T., Tauxe, L., 1993. Geomagnetic palaeointensities during the Cretaceous normal superchron measured using submarine volcanic glass. Nature 366, 238–242.
Pressling, N., Laj, C., Kissel, C., Champion, D., Gubbins, D., 2006. Palaeomagnetic intensities from 14C-dated lava flows on the Big Island, Hawaii: 0–21 kyr. Earth Planet. Sci. Lett. 247, 26–40.
Pressling, N., Brown, M.C., Gratton, M.N., Shaw, J., Gubbins, D., 2007. Microwave palaeointensities from Holocene age Hawaiian lavas: investigation of magnetic properties and comparison with thermal palaeointensities. Phys. Earth Planet. Inter. 162, 99–118.
Pressling, N., Trusdell, F.A., Gubbins, D., 2009. New and revised 14C dates for Hawaiian surface lava flows: paleomagnetic and geomagnetic implications. Geophys. Res. Lett. 36, L11306. http://dx.doi.org/10.1029/2009GL037792.
Riisager, P., Riisager, J., 2001. Detecting multidomain magnetic grains in Thellier palaeointensity experiments. Phys. Earth Planet. Inter. 125, 111–117.

Schweitzer, C., Soffel, H.C., 1980. Paleointensity measurements on postglacial lavas from Iceland. J. Geophys. 47, 57–60.
Selkin, P.A., Tauxe, L., 2000. Long-term variations in palaeointensity. Philos. Trans. R. Soc. London A 358, 1065–1088.
Shaar, R., Tauxe, L., 2013. Thellier GUI: an integrated tool for analyzing paleointensity data from Thellier-type experiments. Geochem. Geophys. Geosyst. 14, 677–692. http://dx.doi.org/10.1002/ggge.20062.
Shaar, R., Ron, H., Tauxe, L., Kessel, R., Agnon, A., 2011. Paleomagnetic field intensity derived from non-SD: testing the Thellier IZZI technique on MD slag and a new bootstrap procedure. Earth Planet. Sci. Lett. 310, 213–224.
Shaw, J., 1974. A new method of determining the magnitude of the palaeomagnetic field, application to five historic lavas and five archaeological samples. Geophys. J. R. Astron. Soc. 39, 133–141.
Stanton, T., Riisager, P., Knudsen, M.F., Thoardrson, T., 2011. New paleointensity data from Holocene Icelandic lavas. Phys. Earth Planet. Inter. 186 (1–2), 1–10. http://dx.doi.org/10.1016/j.pepi.2011.01.006.
Stuiver, M., Reimer, P.J., Reimer, R.W., 2009. CALIB 6.0 program and documentation. Available from: <http://calib.qub.ac.uk/calib> (March 2012).
Tanaka, H., Kono, M., 1991. Preliminary results and reliability of palaeointensity studies on historical and 14C dated Hawaiian lavas. J. Geomagn. Geoelec. 43, 375–388.
Tanaka, H., Kono, M., Kaneko, S., 1995. Paleosecular variation of direction and intensity from two Pliocene-Pleistocene lava sections in Southwestern Iceland. J. Geomag. Geoelec. 47, 89–102.
Tanaka, H., Hashimoto, Y., Morita, N., 2012. Palaeointensity determinations from historical and Holocene basalt lavas in Iceland. Geophys. J. Int. 189, 833–845. http://dx.doi.org/10.1111/j.1365-246X.2012.05412.x.
Tauxe, L., 2009. Essentials of Paleomagnetism. University of California Press, Berkeley.
Tauxe, L., Staudigel, H., 2004. Strenght of the geomagnetic field in the Cretaceous Normal Superchron: new data from submarine basaltic glass of the Troodos Ophiolite. Geochem. Geophs. Geosyst. 5(5), Q02H06. doi:10.1029/2003GC000635.
Tauxe, L., Yamazaki, T., 2007. Paleointensities. In: M. Kono (Ed.), Treatise on Geophysics, Treat. Geophys. 5, 509–563 (Elsevier, New York).
Tauxe, L., Mullender, T.A.T., Pick, T., 1996. Potbellies, waspwaists, and superparamagnetism in magnetic hysteresis. Geophys. Res. 101, 571–583.
Tauxe, L., Bertram, N.H., Seberino, C., 2002. Physical interpretation of hysteresis loops: Micromagnetic modeling of fine particle magnetite, Geochem. Geophs. Geosyst. 3(10). doi:10.1029/2001GC000241.
Tema, E., Kondopoulou, D., 2011. Secular variation of the Earth's magnetic field in the Balkan region during the last eight millennia based on archaeomagnetic data. Geophys. J. Int. 186, 603–614.
Tema, E., Morales, et al.Goguitchaichvili, A., Camps, P., 2013. New archaeointensity data from Italy and geomagnetic field intensity variation in the Italian Peninsula. Geophys. J. Int. 193, 603–614.
Thellier, E., Thellier, O., 1959. Sur l'intensité du champ magnétique terrestre dans le passé historique et géologique. Annal. Géophys. 15, 285–376.
Tsunakawa, H., Shaw, J., 1994. The Shaw method of paleointensity determinations and its application to recent volcanic rocks. Geophys. J. Int. 118, 781–787.
Valet, J.P., Herrero-Barvera, E., 2000. Paleointensity experiments using alternating field demagnetization. Earth Planet. Sci. Lett. 177, 43–58.
Valet, J.P., Herrero-Bervera, E., Carlut, J., Kondopoulou, D., 2010. A selective procedure for absolute paleointensity in lava flows. Geophyis. Res. Lett. 37, L16308. http://dx.doi.org/10.1029/2010GL044100.
Xu, S., Dunlop, D.J., 1995. Theory of partial thermoremanent magnetization in multidomain grains. 2. Effect of microcoercivity distribution and comparison with experiment. J. Geophys. Res. 99, 9025–9033.
Xu, S., Dunlop, D.J., 2004. Thellier paleointensity theory and experiments for multidomain grains. J. Geophys. Res. 109, B07103. http://dx.doi.org/10.1029/2004JB003024.
Yamamoto, Y., Tsunakawa, H., Shibuya, H., 2003. Palaeointensity study of the 1960 Hawaiian lava: implications for possible causes of erroneously high intensities. Geophys. J. Int. 153, 263–276.
Yu, Y., Tauxe., L., 2005. Testing the IZZI protocol of geomagnetic field intensity determination, Geoch. Geophs. Geosyst. 6 (5), Q05H17. doi: 10.1029/2004GC000840.
Yu, Y., Tauxe, L., Genevey, A., 2004. Toward an optimal geomagnetic field intensity determination technique, Geochem. Geophs. Geosyst. 5 (2), Q02H07. doi: 10.1029/2003GC000630.